

Supplementary Materials

MIL-100(Fe)-catalyzed efficient conversion of hexoses to lactic acid

Shan Huang, Kai-Li Yang, Xiao-Fang Liu, Hu Pan, Heng Zhang and Song Yang,*

State Key Laboratory Breeding Base of Green Pesticide & Agricultural Bioengineering, Key Laboratory of Green Pesticide & Agricultural Bioengineering, Ministry of Education, State-Local Joint Laboratory for Comprehensive Utilization of Biomass, Center for Research & Development of Fine Chemicals, Guizhou University, Guiyang 550025, China. Email: jhzx.msm@gmail.com, Tel: +86(851)8829-2171, Fax: +86(851)8829-2170.

Table contents

Catalyst preparation and characterization

Synthesis of MIL-100(Fe)

Synthesis of Cu-BTC

Synthesis of MIL-100(Cr)

Regeneration of the recovered catalyst

Fig. S1. DFT pore size distribution plots of the synthesized MIL-100(Fe).

Fig. S2. XRD patterns of the synthesized (a) Cu-BTC and (b) MIL-100(Cr).

Fig. S3. The FT-IR spectra of Cu-BTC and MIL-100(Cr).

Fig. S4. Py-FT-IR spectra of the synthesized MIL-100(Fe), Cu-BTC and MIL-100(Cr).

Fig. S5. XRD patterns of the fresh and the recovered MIL-100(Fe).

Fig. S6. FT-IR spectra of the synthesized and the recovered MIL-100(Fe).

Fig. S7. N₂ isotherm (a) and DFT pore size distribution plots (b) of the the recovered MIL-100(Fe).

Fig. S8. NH₃-TPD profiles of the fresh and the recovered MIL-100(Fe).

Fig. S9. FT-IR spectra of the fresh MIL-100(Fe) and the one after regeneration

Fig. S10. Typical chromatogram of lactic acid (a), chromatogram of mixed authentic compounds containing equal amounts of lactic acid (b), typical chromatogram of levulinic acid (c), and chromatogram of mixed authentic compounds containing equal amounts of levulinic acid (d)

Table S1 Catalytic results obtained for sugar conversion with MIL-100(Fe). Showing yields to methyl lactate (ML), pyruvaldehyde dimethyl acetal (PADA), non-identified products (n.i.p.), and not detect (N.D.).

Catalyst preparation and characterization

Synthesis of MIL-100(Fe)

MIL-100(Fe) was prepared according to the literature.⁵¹ The reactant mixture was loaded as the composition of 1.0 Fe^o : 0.67 1,3,5-BTC : 2.0 HF : 0.6 HNO₃ : 277 H₂O (1,3,5-BTC=1,3,5-benzenetricarboxylic acid or trimesic acid) in a Teflon autoclave. Then the Teflon autoclave was heated up to 150 °C and kept at this temperature for 12 h. After the hydrothermal reaction, the light orange solid product was recovered by filtration, washed with deionized water. The as synthesized MIL-100(Fe) was further purified by deionized water at 80 °C for 5 h to decrease the amount of residual unreacted ions (typically, 1 g of MIL-100(Fe) in 350 ml of water) and then ethanol at 60 °C for 3 h until no detection of colored impurities in the mother liquor solution, resulting in the highly purified MIL-100(Fe). The solid was finally dried overnight at 80 °C in air.

Synthesis of Cu-BTC

Cu-BTC was prepared according to the literature.⁵² 1.75 g of Cu(NO₃)₂·3H₂O and 0.84 g of trimesic acid were dissolved in a mixture of 24 mL of water and 24 mL of EtOH. The suspension was heated for 14 h at 120 °C in a Teflonlined autoclave. At the end of the reaction, the autoclave was cooled down to room temperature, and the resulting blue powder was filtered off and washed once with water and then a second time with EtOH. Thereafter, the sample was dried under vacuum at 100 °C for 12 h and then kept under nitrogen atmosphere until further use.

Synthesis of MIL-100(Cr)

MIL-100(Cr) was prepared according to the literature.⁵³ 1.200 g CrO₃ (12.00 mmol), 2.520 g H₃BTC (11.99 mmol), 0.42 mL HF (12 mmol; 48-51 % in H₂O) and 58 mL of deionized water were placed in a 100 mL Teflon-liner. The Teflon-liner was placed in an autoclave and heated to 200 °C within 2 h. After 96 h the autoclave was cooled to room temperature within 2 h. The green powder was filtered, washed with deionized water (2 x 30 mL) and dried in air for 20 h. For activation the powder was first stirred for 4 h in 140 mL DMF at 383 K, then additional 16 h at room temperature. After filtration and stirring for 5 h in 100 mL EtOH at 333 K, the green powder was centrifuged and stirred again for 20 h in 200 mL of deionized water at 363 K. After centrifugation the solid was dried in air.

Regeneration of the recovered catalyst

We employed a simple method for regeneration of the recovered catalyst (after reusing for 4 times), referring to the protocol reported by Han *et al.*⁵⁴, wherein the recovered catalyst was dissolved into HF and HNO₃ solution with the addition of H₃BTC. The solution was kept in an oven at 150 °C for 12 h, purified by deionized water at 80 °C and ethanol at 60 °C. The solid was finally dried overnight at 80 °C in air. Because the acidic solution of an MOF contained metal ions and little organic ligands, an extra addition of ligand could lead to the regeneration of a pristine MOF.

The characterization techniques used for the Cu-BTC and MIL-100(Cr) were same with MIL-100(Fe).

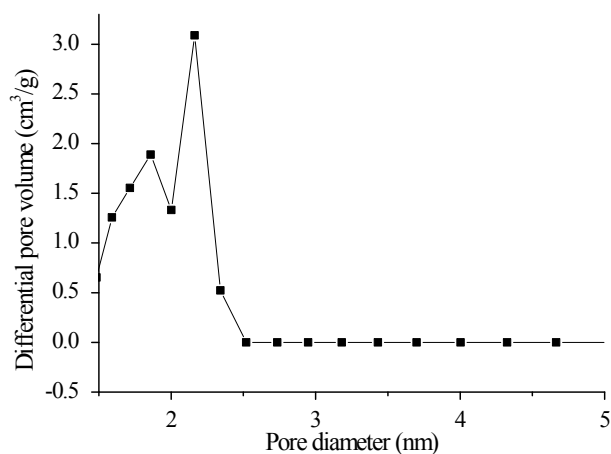


Fig. S1. DFT pore size distribution plots of the synthesized MIL-100(Fe).

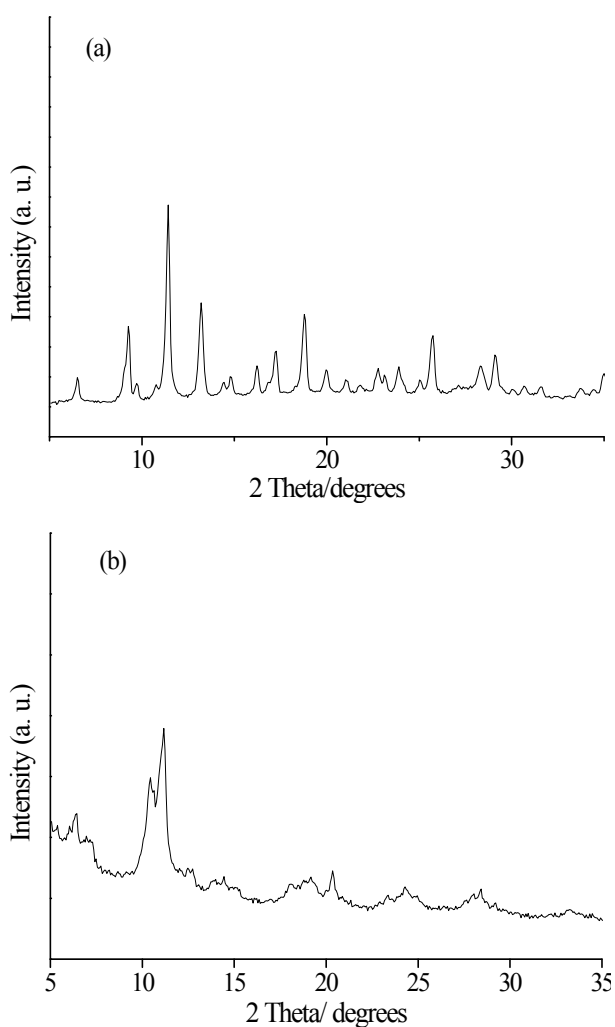


Fig. S2. XRD patterns of the synthesized (a) Cu-BTC and (b) MIL-100(Cr).

The experimental XRD patterns (Fig.S2) of the synthesized MIL-100(Cr) and Cu-BTC are in good agreement with the one in references, showing the successful

preparation of these two materials.

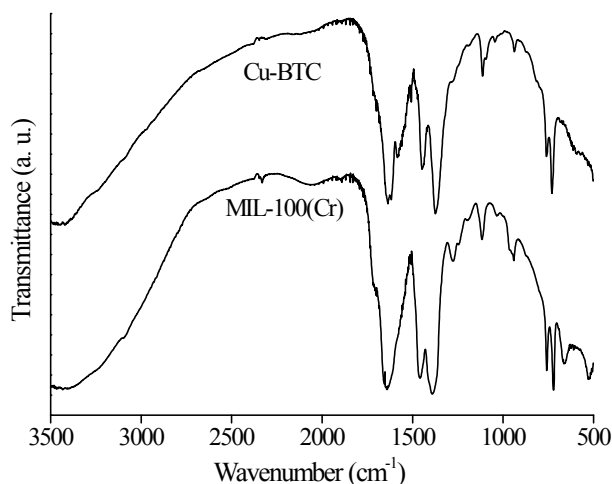


Fig. S3. The FT-IR spectra of Cu-BTC and MIL-100(Cr)

There is no peak at 1710-1720 cm⁻¹ (the C=O stretching vibration at 1710-1720 cm⁻¹ is assigned to residual H₃BTC) indicates that the purification procedure used here is particularly effective to remove residual H₃BTC. The bands around 729 and 1450 cm⁻¹ are due to (C-H) bending and a combination of benzene ring stretching and deformation.

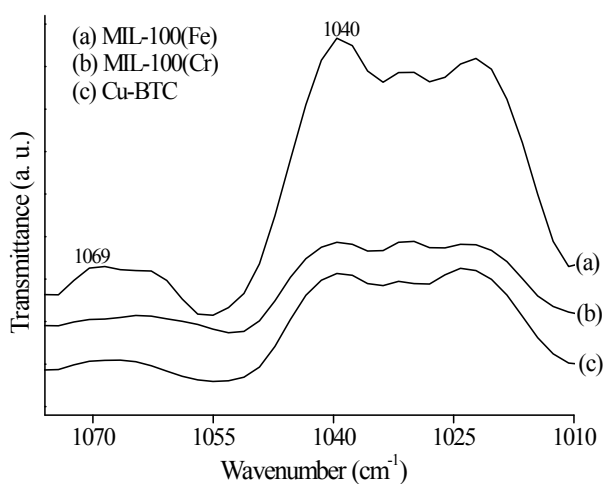


Fig. S4. Py-FT-IR spectra of the synthesized MIL-100(Fe), Cu-BTC and MIL-100(Cr).

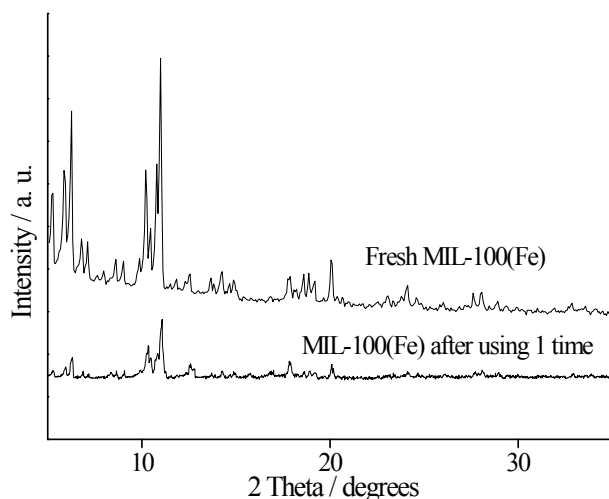


Fig. S5. XRD patterns of the fresh and the recovered MIL-100(Fe).

Fig. S5 shows that the XRD pattern of the recovered MIL-100(Fe) maintained almost no change, verifying the stability of the structure and the active sites, which explained that MIL-100(Fe) was relatively stable .

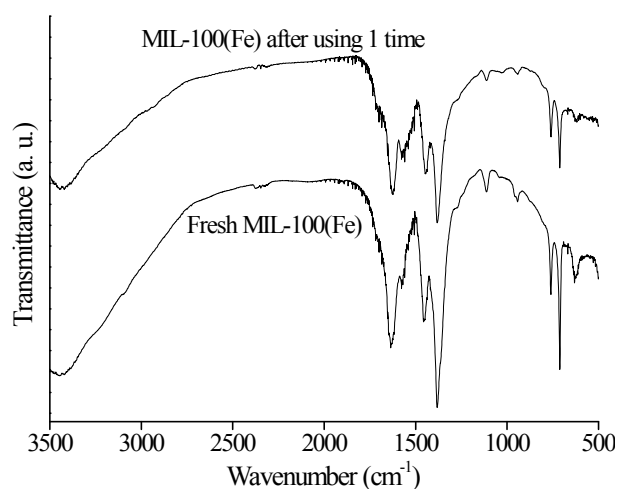


Fig. S6. FT-IR spectra of the synthesized and the recovered MIL-100(Fe).

Fig. S6 shows the FT-IR spectra of the synthesized and the recovered MIL-100(Fe). As we can see that the material still remained its characteristic functional groups, which means good reusability of MIL-100(Fe).

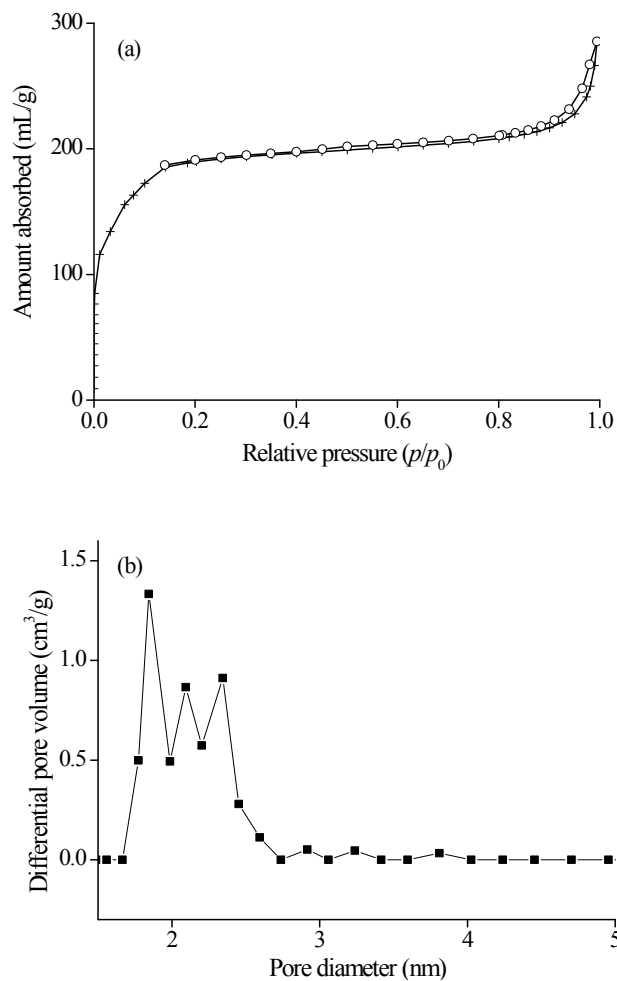


Fig. S7. N₂ isotherm (a) and DFT pore size distribution plots (b) of the recovered MIL-100(Fe).

As we can see from Fig. S7, the recovered MIL-100(Fe) gave a BET surface area of 709 m²/g with a pore volume of 0.44 cm³/g.

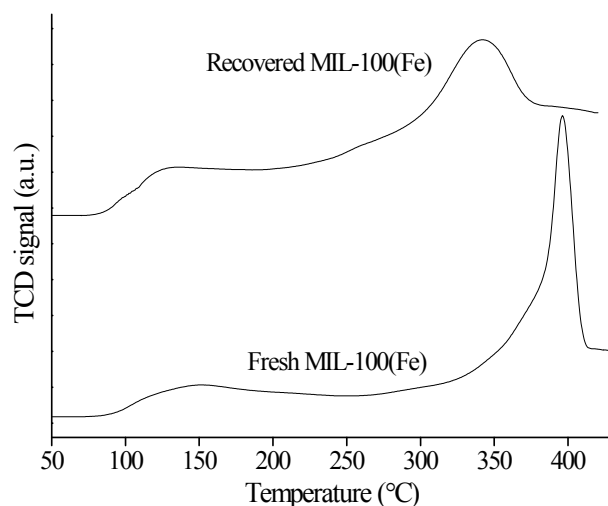


Fig. S8. NH_3 -TPD profiles of the fresh and the recovered MIL-100(Fe).

The difference in acidity of the fresh and recovered materials was evaluated based on the TPD of NH_3 , from Fig. S8, we can see that there are NH_3 desorption peaks resulting from the physical and chemical adsorption on Brønsted or Lewis acid sites.⁵⁵ The broad peaks ranging from 80 to 250 °C demonstrated the existence of weak-to-medium acid sites, while 250 to 420 °C corresponded to strong acid sites on the surface of catalyst, respectively,^{55, 56} and the total amount of acid sites was 3.92 and 3.57 mmol/g for the fresh and the recovered materials, respectively. There was only a slight decrease in acidity of catalyst.

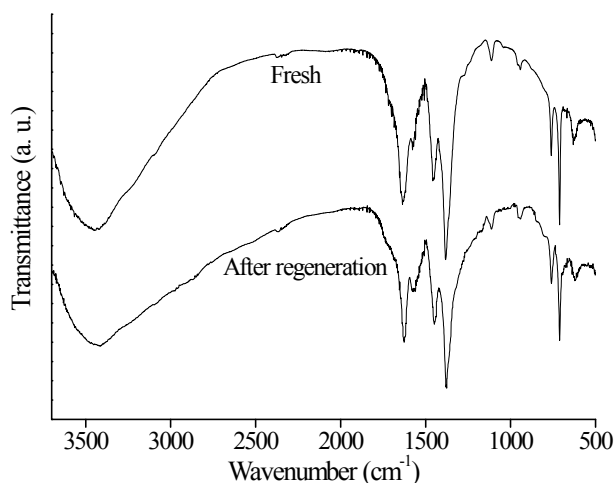


Fig. S9. FT-IR spectra of the fresh MIL-100(Fe) and the one after regeneration

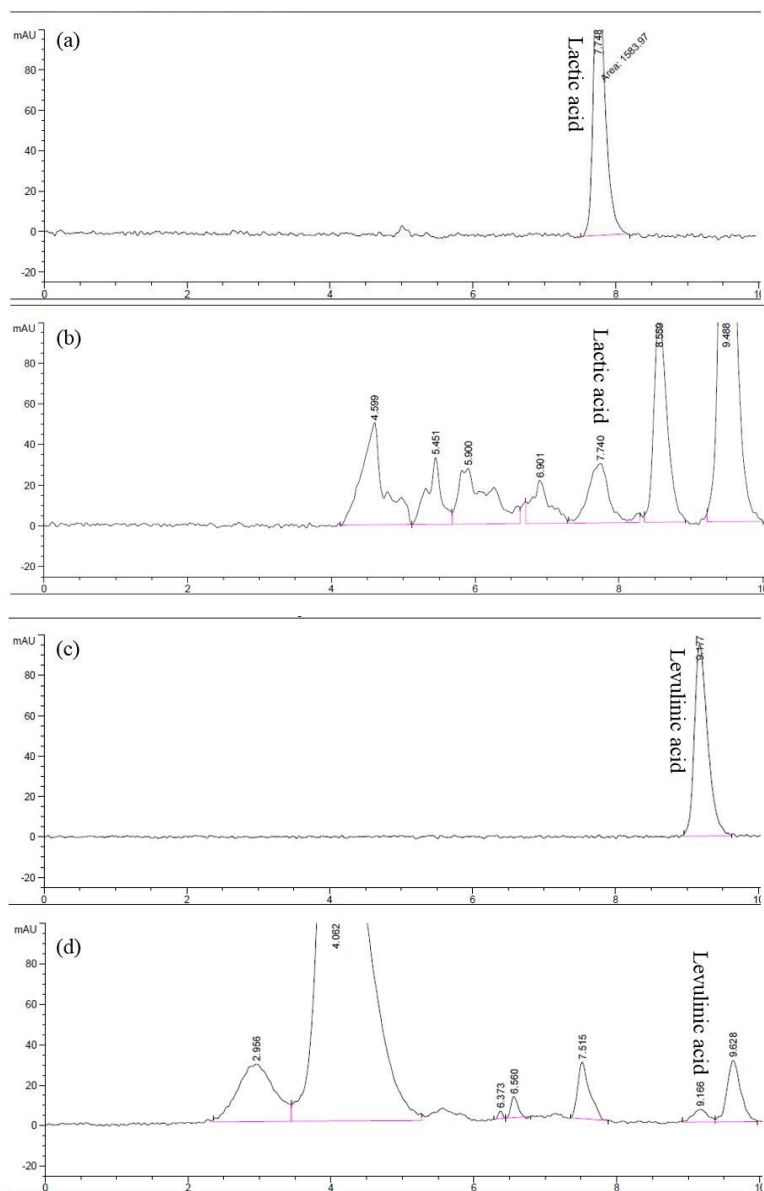


Fig. S10. Typical chromatogram of lactic acid (a), chromatogram of mixed authentic compounds containing equal amounts of lactic acid (b), typical chromatogram of levulinic acid (c), and chromatogram of mixed authentic compounds containing equal amounts of levulinic acid (d)

Table S1 Catalytic results obtained for sugar conversion with MIL-100(Fe). Showing yields to methyl lactate (ML), pyruvaldehyde dimethyl acetal (PADA), non-identified products (n.i.p.), and not detect (N.D.).

Entry	substrate	catalyst	T (°C)	t (h)	Yields (%)			Total yield (%)	conversion (%)
					MLA	PADA	n.i.p.		
1	fructose	blank	180	28	3	1	4	8	76
2	fructose	MIL-100(Fe)	180	8	17	0	2	19	79
3	fructose	MIL-100(Fe)	180	18	29	0	1	30	80
4	fructose	MIL-100(Fe)	180	28	33	1	3	37	80
5	fructose	MIL-100(Fe)	180	38	26	1	6	33	80
6	fructose	MIL-100(Fe)	140	28	7	0	6	13	78
7	fructose	MIL-100(Fe)	160	28	9	0	1	10	78
8	fructose	MIL-100(Fe)	200	28	29	0	3	32	80
9	glucose	MIL-100(Fe)	180	28	3	0	1	4	N.D.
10	sucrose	MIL-100(Fe)	180	28	12	0	1	13	N.D.
11	cellulose	MIL-100(Fe)	180	28	6	0	1	7	N.D.
12	inulin	MIL-100(Fe)	180	28	16	0	4	20	N.D.

Reaction conditions: 0.05 g MIL-100(Fe), 0.05 g substrate, 10 mL MeOH.

References:

- S1 J. W. Yoon, Y. K. Seo, Y. K. Hwang, J. S. Chang, H. Leclerc, S. Wuttke, P. Bazin, A. Vimont, M. Daturi, E. Bloch, P. L. Llewellyn, C. Serre, P. Horcajada, J. M. Grenèche, A. E. Rodrigues, G. Férey, *Angew. Chem. Int. Ed.*, 2010, **49**, 5949.
- S2 M. Hartmann, S. Kunz, D. Himsl, O. Tangermann, *Langmuir*, 2008, **24**, 8634.
- S3 M. Wickenheisser, F. Jeremias, S. K. Henninger, C. Janiak, *Inorg. Chim. Acta*, 2013, **407**, 145.
- S4 S. Han, M. S. Lah, *Cryst. Growth Des.*, 2015, **15**, 5568.
- S5 W. Zhang, Y. Shi, C. Y. Li, Q. D. Zhao, X. Y. Li, *Catal. Lett.*, 2016, **146**, 1956.
- S6 D. W. Kim, H. G. Kim, D. H. Cho, *Catal. Commun.*, 2016, **73**, 69.

